Regional benthic $\delta^{18}O$ stacks for the "41-kyr world" - an Atlantic-Pacific divergence between 1.8-1.9 Ma

Yuxin Zhou, Lorraine E. Lisiecki, Taehee Lee, Geoffrey Gebbie, and Charles Lawrence

Key points

- New Atlantic and Pacific benthic $\delta^{18}O$ stacks show different patterns between 1.8-1.9 Ma.
- The Atlantic-Pacific difference in this portion of the 41-kyr world may be caused by regional sensitivity to relatively strong precession.
- Regional benthic $\delta^{18}O$ stacks are preferable to global stacks for stratigraphic alignment.

Abstract

Benthic $\delta^{18}O$ stacks are the benchmarks by which paleoceanographic data are stratigraphically aligned and compared. However, a recent study found that between 1.8-1.9 million years ago (Ma) several Ceara Rise records differed substantially from the widely used LR04 global stack. Here, we use new Bayesian stacking software to construct regional stacks and demonstrate a geographical divergence in benthic $\delta^{18}O$ features from 1.8-1.9 Ma. The pattern of isotopic stage features observed in the Ceara Rise is widespread throughout the Atlantic and differs notably from Pacific records. We propose that this regional difference in isotopic stages may be the result of relatively strong precession forcing and weaker obliquity forcing between 1.8-1.9 Ma. In accordance with the Antiphase Hypothesis, our results highlight a period of apparent sensitivity to regional precession forcing that is masked during most of the 41-kyr world due to the amplitude modulation of obliquity forcing.

Plain language summary

To determine the age of deep-sea sediments, often the oxygen isotope ratios of microfossils are measured and compared to a previously compiled global benchmark. Recently, one of the most widely used oxygen isotope benchmarks has been challenged based on a comparison with several Atlantic records. In this study we assess several lines of evidence including utilizing newly available data and software. We confirm the challenge to the global oxygen isotope benchmark and find that it is more widespread than originally realized. Particularly, we find that oxygen isotope records display different patterns between the Atlantic and Pacific Oceans from 1.8-1.9 million years ago (Ma). We propose that this difference is the result of the opposing seasonal solar radiation anomalies received by the northern and southern hemispheres, which exhibited particularly large amplitudes during this time. Our study adds supporting evidence to a hypothesis that explains the dominant frequency of climatic cycles from 1.2-2.6 Ma.

Introduction

Benthic $\delta^{18}O$ stacks set benchmarks for comparison of paleoceanographic data (e.g., Ahn et al., 2017; Lisiecki & Raymo, 2005; Martinson et al., 1987) and are used to evaluate ice sheet evolution and climate responses to orbital forcing (Lisiecki, 2010; Lisiecki & Raymo, 2007; Raymo et al., 2006). The global "LR04" Plio-Pleistocene stack is one of the most commonly used benthic $\delta^{18}O$ stacks (Lisiecki & Raymo, 2005). Given its wide use, the accuracy of LR04, even in relatively minor details, has important implications for a broad range of paleoceanographic applications.

Style Definition: Caption

Deleted: thoroughly

Deleted: opposite

Commented [LL1]: My preference is to cite papers in chronological order (older before more recent ones)

Commented [YZ2R1]: AGU style guide sorts citations alphabetically

Wilkens et al. (2017) identified 1.8-1.9 Ma as a period where LR04 differs significantly from a benthic $\delta^{18}O$ record stack from five Ceara Rise cores. The Ceara Rise stack exhibits fewer glacial cycles compared to LR04 during 1.8-1.9 Ma, casting doubt on how globally representative LR04 was during the early Pleistocene. Wilkens et al. (2017) attributed the discrepancy to LR04's choice of the initial alignment target records, ODP (Ocean Discovery Program) sites 677 and 849. Sites 677 and 849 use splicing to construct continuous records from adjacent drill holes, a common practice for achieving complete recovery at ODP sites. Problems with splicing, Wilkens et al. contended, might have made sites 677 and 849 records inaccurate.

Several recent advances provide us with an opportunity to place in a broader context the discrepancy with LR04 found by Wilkens et al. (2017). First, newly developed software for stacking benthic $\delta^{18}O$ records requires fewer input records and enables us to efficiently construct regional stacks (Lee and Rand et al., 2023), which can reveal spatial variability that is otherwise masked in global stacks (Lisiecki & Raymo, 2009; Lisiecki & Stern, 2016; Skinner & Shackleton, 2005; Stern & Lisiecki, 2014). We can thus assess whether the pattern seen in the Ceara Rise stack is representative of regional or global changes. Second, the subsequent publication of higher-resolution Atlantic records, e.g., Hodell and Channell (2016), allows an investigation into the 1.8-1.9 Ma period with less ambiguity. Third, the observation of a Laurentide meltwater event during the 1.8-1.9 Ma period (Shakun et al., 2016) points to a potential mechanistic explanation for the Ceara Rise $\delta^{18}O$ signal identified by Wilkens et al. Here, we apply these new data and techniques to demonstrate that the 1.8-1.9 Ma period stands out as an unusual instance of regional divergence in Pleistocene benthic $\delta^{18}O$. We discuss the mechanisms that could have caused this divergence and implications for the LR04 stack.

Methods

We construct the new Pleistocene regional Atlantic and Pacific Pleistocene stacks using 209 benthic $\delta^{18}O$ records, including 55 records from LR04 (Lisiecki & Raymo, 2005), 132 additional records from the ProbStack (Ahn et al., 2017), and 22 recently published records identified by this study (Table S1; Fig. S1-2). Many of the newly added records have relatively high resolutions, resulting in a 48% increase in data points compared to the ProbStack (Figs. S1-2). Over the Pleistocene, the Pacific stack includes data from 80 cores while the Atlantic stack includes data from 119 cores. To evaluate the hypothesis of Wilkens et al. (2017), we also construct shorter regional stacks for the Atlantic and the Pacific from 1.5 to 2.1 Ma. Between 1.8-1.9 Ma, there are 14 Pacific cores and 25 Atlantic cores. An Indian Ocean stack was not constructed because only one record is available from the Indian Ocean during 1.8-1.9 Ma.

The new stacks are created using Bayesian Inference Gaussian Process regression and Multiproxy Alignment for Continuous Stacks (BIGMACS), which is a newly developed software package for probabilistically stacking ocean sediment core data and constructing multiproxy age models (Lee and Rand et al., 2023). Unlike other probabilistic benthic $\delta^{18}O$ alignment software (Ahn et al., 2017; Lin et al., 2014), BIGMACS can reliably construct benthic $\delta^{18}O$ stacks using a smaller number of cores because it estimates a time-continuous signal using Gaussian process regression (Rasmussen & Williams, 2005). This enhances our ability to create and compare benthic $\delta^{18}O$ stacks for the Atlantic and the Pacific back to the early Pleistocene (see below). Another advancement of BIGMACS is that it probabilistically integrates additional depth-age

Deleted: [

Deleted:]

Commented [LL3]: Add a supplemental table with the core location and citation info

Deleted: [

Deleted:]

estimates provided by the user. Here we incorporate age estimates from the Neptune Sandbox Berlin (NSB) database (Renaudie et al., 2020), which compiled biostratigraphic and paleomagnetic events from the International Ocean Discovery Program (IODP) and its predecessors. The conversion of NSB hole-specific meters below sea floor (mbsf) depths to meters composite depth (mcd) was done using the IODP Janus Depth Point Calculator. Because the age information provided by the NSB database does not come with uncertainty estimates, we conservatively specify the age uncertainty as Gaussian distributions with a standard deviation of 100 kyr.

BIGMACS stack construction requires an initial alignment target, for which we used the LR04 global stack (Lisiecki & Raymo, 2005). However, because the LR04 stack may not be a good representation of $\delta^{18}O$ variability from 1.8-1.9 Ma, its use as an initial alignment target could be problematic. For the 1.5-2.1 Ma stacks, we assigned additional age control points in BIGMACS for records that have sufficient resolution by visually identifying the glacial maxima associated

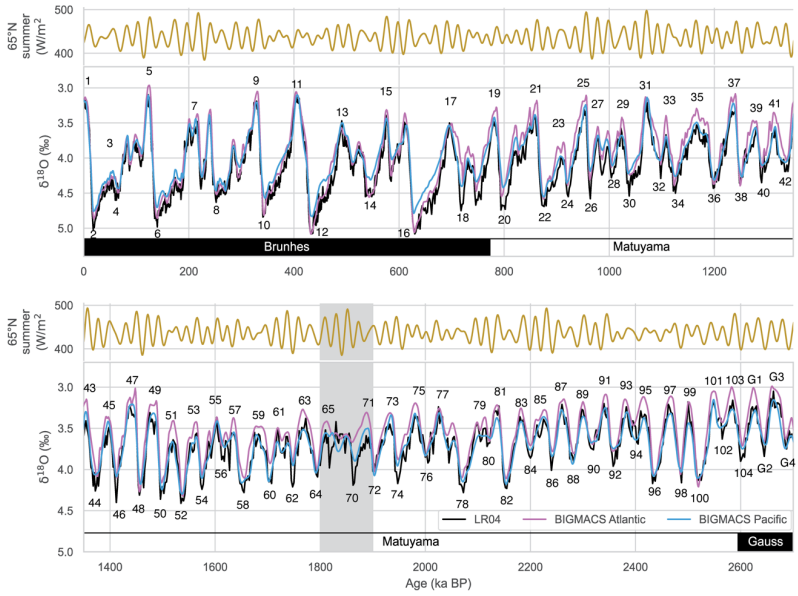

Figure 1. BIGMACS regional Pleistocene stacks for the Pacific (blue) and Atlantic (purple) without added tie points. The results presented are the stack means. Also shown is the LR04 global stack (black). The gray area is the 1.8-1.9 Ma period when the two BIGMACS regional stacks diverge. Also shown on top is the summer insolation at 65 °N. The numbers mark the Marine Isotope Stages. The black and white rectangles denote the geomagnetic chrons.

with MIS 64 and 74 and assigning them ages based on the respective obliquity minima (1.793 and 1.958 Ma). Because of the disagreement particularly between the LR04 global stack with the Atlantic records, we additionally identified the glacial maxima associated with MIS 68 and 70 in the Atlantic records that have sufficient resolution and assigned them ages based on the respective insolation minima (1.841 and 1.864 Ma) setting the BIGMACS built-in "additional_ages" parameter with an one-kyr standard deviation. In assigning ages, we are guided by the average normalized sedimentation rate to ensure it is relatively smooth and does not have outliers (Text S1, Fig. S3-6). We do not propose that these age assignments are necessarily appropriate corrections to the MIS ages of the LR04 stack; we merely use them to ensure consistent alignments in BIGMACS where fit to the original LR04 stack is poor. (MIS 66 was not used because it was poorly defined in most high-resolution records.) The discrepancies in the regional stacks between 1.8-1.9 Ma can also be seen in the full Pleistocene stacks for

Deleted: , 68, 70,

Deleted: 2

Deleted: , 1.837, 1.878,

Deleted: 17

which we did not set any additional age controls (Text S2 and Fig. 1); however, the assigned age control points do affect the glacial-interglacial features of the regional stacks from 1.8-1.9 Ma (Fig. 2).

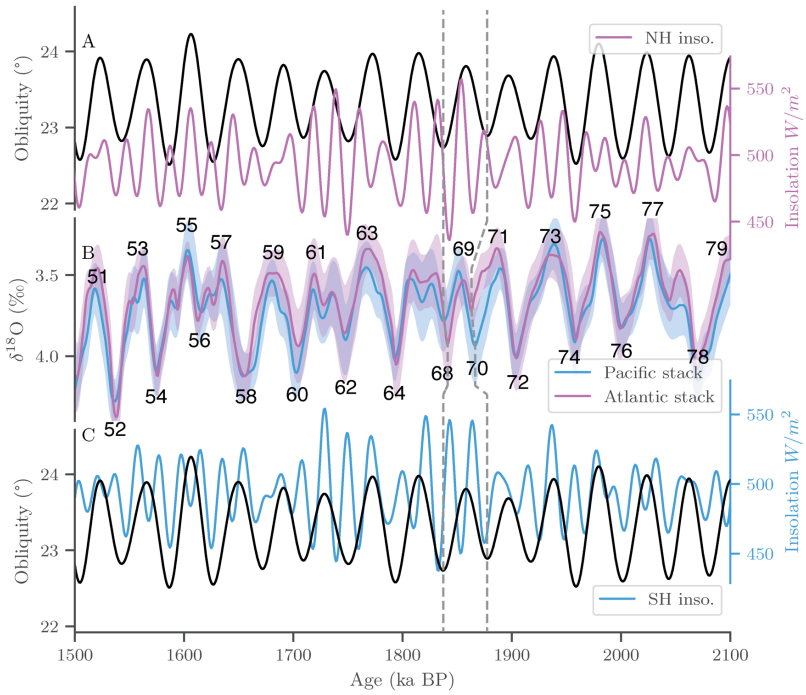

Figure 2. BIGMACS Atlantic and Pacific regional stacks compared to orbital parameters. (A) Obliquity (black) and summer insolation at 65°N (purple). (B) BIGMACS Atlantic (purple) and Pacific (blue) regional stacks. Shading denotes the 1σ uncertainty of the stack $\delta^{18}O$ values. (C) Obliquity (black) and summer insolation at 65°S (blue). The vertical dashed lines associate glacial periods in the regional benthic $\delta^{18}O$ stacks with the corresponding obliquity minimums.

Deleted: represent the additional age control points used in the BIGMACS stack construction runs in records with adequate resolution and discernable regional trends

Can we detect the same Atlantic-Pacific difference in the classic LR04 stack (Lisiecki & Raymo, 2005)? We separated the input records of LR04 based on ocean basins using the same $\delta^{18}O$ data on the age models used to construct the LR04 stack and binned at the same 2.5-kyr resolution used for the LR04 stack from 1.5-3 Ma. We refer to these results as the LR04 Atlantic/Pacific binned stacks.

Results

The Atlantic and Pacific stacks, for the most part, closely follow each other except at a few places, notably during 1.8-1.9 Ma (Fig. 2). At ~1.863 Ma (MIS 70), the glacial maximum is much stronger in the Pacific stack than the Atlantic stack. In comparison to other glacial maxima from 1.5-2.1 Ma, the Atlantic benthic $\delta^{18}O$ response at MIS 70 more closely resembles a cold isotopic substage within a long interglacial than a glacial maximum. In contrast, the Atlantic stack's glacial maximum at ~1.841 Ma (MIS 68) is stronger than in the Pacific stack. Neither of the regional stacks reproduces the pattern in LR04 or ProbStack during this period. LR04 shows two poorly resolved glacial intervals (MIS 66 and 68) between two relatively normal glacial maxima (MIS 64 and 70); in contrast, the new Atlantic stack has a very weak MIS 70 while MIS 68 is similar in magnitude to MIS 64 and 72. Another Atlantic-Pacific difference appears at ~2.05 Ma during the transition from glacial MIS 78 to interglacial MIS 77; at this time the Atlantic stack shows a stronger interglacial substage (similar to LR04) than the Pacific stack.

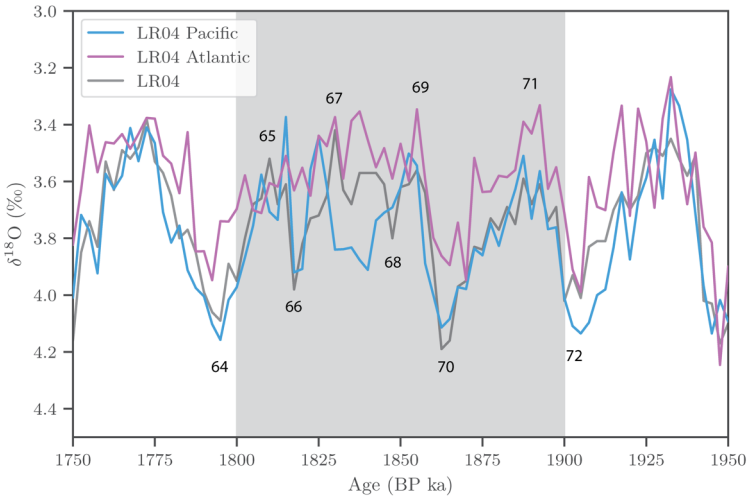

Figure 3. The LR04 global stack and separate binned stacks of its component Atlantic and Pacific records (as aligned during LR04 stack construction). The gray shade outlines the 1.8-1.9 Ma period where the Atlantic and the Pacific binned stacks diverge. Numbers denote the Marine Isotope Stages 64-72 in LR04.

Like the regional BIGMACS stacks, the LR04 Atlantic and Pacific binned stacks differ from one another between 1.8-1.9 Ma (Fig. 3). MIS 66 and 68 are absent in the LR04 Atlantic binned stack, whereas the Pacific binned stack matches LR04 well. Discrepancy in the relative amplitudes of MIS 68 and 70 between the Atlantic stacks produced by BIGMACS and LR04 binning may be caused by alignment errors during LR04 construction associated with relatively low resolution Atlantic records. The new BIGMACS Atlantic stack contains more than double the $\delta^{18}O$ measurements than the LR04 Atlantic binned stack from 1.8-1.9 Ma.

Deleted: 78

Deleted: 37

Deleted: The LR04 Pacific binned stack matches LR04 well, whereas MIS 66 and 68 are absent in the Atlantic binned stack. …

Deleted: 123% more

Formatted: Font: (Default) Times New Roman, 12 pt

Discussion

In both the BIGMACS regional stacks and LR04 region-specific binned stacks, Pacific benthic $\delta^{18}O$ exhibits a different pattern of variability than the Atlantic between 1.8-1.9 Ma. Although benthic $\delta^{18}O$ is often considered a well-mixed proxy for global ice volume, one possible explanation for the regional difference in benthic $\delta^{18}O$ during this period may be the differences in the deep water temperature or salinity in the two ocean basins. For example, the physical properties of Pacific Deep Water may have been sensitive to southern hemisphere (SH) insolation while Atlantic deep water responded to northern hemisphere (NH) insolation. In such a scenario, the opposite phase of precession effects on hemispheric seasonal insolation could produce differences between Atlantic and Pacific benthic $\delta^{18}O$.

Despite orbital insolation during the late Pliocene/early Pleistocene being dominated by precession (Fig. 4), benthic $\delta^{18}O$ records exhibit strong 41-kyr obliquity cycles. This mismatch between the substantial role that precession played in modulating the NH summer insolation and the apparent lack of a precessional imprint in geological records is termed the "41-kyr problem" (Raymo & Nisancioglu, 2003; Watanabe et al., 2023). Many researchers have put forward theories on why the 41-kyr world is dominated by obliquity. Among them, the Antiphase Hypothesis has particular appeal to explain our observations (Morée et al., 2021; Raymo et al., 2006). The Antiphase Hypothesis proposes that opposing responses of the northern and southern hemisphere ice sheets on precessional time scales canceled each other out in the global ice volume signal. For example, while cool NH summers lead to northern ice growth, coeval warm southern hemisphere (SH) summers act to shrink the Antarctic Ice Sheet. Obliquity, which exerts a symmetric effect on both hemispheres, is left as the governing cyclicity of global ice volume during this period.

Deleted: opposite

The Antiphase Hypothesis provides a framework to explain the Atlantic-Pacific difference in benthic $\delta^{18}O$ records during 1.8-1.9 Ma (Fig. 2). While obliquity still paces the glacial-interglacial cycles in global ice volume, the opposite phase of the northern and southern hemisphere insolation on precession time scales could have influenced the magnitudes of glacial benthic $\delta^{18}O$ change in the Atlantic and the Pacific. In particular, the 1.8-1.9 Ma time interval experienced uniquely strong precession and weak obliquity relative to the rest of the 41-kyr world (Fig. 4). While high-latitude summer insolation is always dominated by precession (Raymo & Nisancioglu, 2003), the contrast between the strong precession and weak obliquity during 1.8-1.9 Ma stands out. Other times of similar relative power of obliquity and precession forcing are not directly comparable because they occur before or after the 41-kyr world, e.g., 0.9-1 Ma and 3-3.1 Ma. Before the 41-kyr world, the northern hemisphere was largely ice-free (Sosdian & Rosenthal, 2009). After the 41-kyr world, the Laurentide ice sheet expanded in size and the glacial cycles transitioned to 100-kyr pacing (Lisiecki & Raymo, 2007). The 1.8-1.9 Ma period is, thus, a unique window of time when more precession response might be expected compared to the rest of the 41-kyr world.

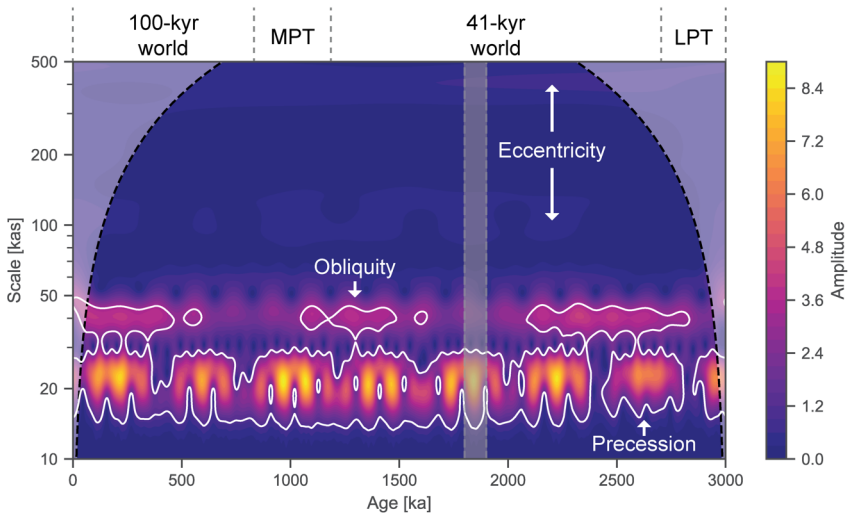

Figure 4. Wavelet spectrum of insolation at 65° N for the Plio-Pleistocene generated with Wavelet Continuous Transform using the Morlet wavelet (Torrence and Compo, 1998). The white lines delineate regions of the spectrum that are significant against a random AR(1) benchmark. The dashed lines denote the 1.8-1.9 Ma period where the Atlantic and Pacific records diverge. LPT: Late Pliocene Transition (Sosdian and Rosenthal, 2009). MPT: Mid-Pleistocene Transition. This figure was generated with Pyleoclim (Khider et al., 2020).

Examining the northern and southern summer insolation forcing from 1.8-1.9 Ma (Fig. 2), we find that the magnitudes of the Atlantic and Pacific glacial responses are likely caused by the hemispheric insolation differences during the obliquity minimum. The obliquity minimum at 1.878 Ma coincided with a maximum in NH summer insolation and minimum SH summer insolation due to the opposite hemispheric effects of precession on seasonal insolation. Thus, NH insolation might be expected to produce a weaker and delayed glacial response in MIS 70 in the northern hemisphere at this time. In the Pacific, MIS 70 might be expected to be strong because SH insolation is low during the obliquity minimum. By the time NH insolation decreases, the relatively high obliquity probably reversed the NH cooling trend quickly. Hemispheric circumstances are reversed during MIS 68 with NH insolation low early during the obliquity minimum (amplifying NH cooling) and the Pacific cooling delayed by a SH insolation peak (initially suppressing SH cooling). However, the SH insolation minimum was not as far offset from the obliquity minimum during MIS 68 as the NH insolation was during MIS 70, so the antiphase effect is weaker for MIS 68.

The response of the Atlantic stack during MIS 70 is similar to MIS 56 (Fig. 2). They are similarly weak glacials and both have NH precession maximum that coincide with the obliquity

Deleted: t

Deleted: In contrast, the obliquity minimum at 1.837 Ma is closely preceded by a strong NH summer insolation minimum and SH summer insolation maximum.

minimum. The interesting difference between the two glacials is that the Pacific matches the Atlantic during MIS 56, in contrast to the strong Pacific glacial maximum during MIS 70. That could be because precession forcing is stronger and obliquity weaker at 1.878 Ma than ~1.6 Ma.

If the temperature or salinity of Pacific Deep Water and North Atlantic Deep Water separately exhibited sensitivity to precession-driven SH and NH summer insolation, respectively, the benthic $\delta^{18}O$ values recorded for the two water masses could differ. For example, Raymo et al. (2006) asserted that the temperature/salinity of the Southern Ocean likely co-varied with the changes in the Antarctic ice volume; such Southern Ocean changes would also be expected to affect Antarctic Bottom Water (AABW) and Pacific Deep Water (PDW). At the same time, the North Atlantic Deep Water (NADW) temperature or salinity signal would likely have had been influenced by the antiphased NH precession signal. The difference in the temperature/salinity signals driven by the timing of precession maxima and minima relative to obliquity can potentially explain the difference in glacial amplitudes. Because of the relatively strong orbital signals in the precession band during this period, the precession effect on the regional benthic $\delta^{18}O$ could have been stronger than for the rest of the 41-kyr world, leaving vestiges of a precession signal in the otherwise obliquity-dominated benthic $\delta^{18}O$ signals.

Circulation reconstructions for the 41-kyr world find that the Atlantic was primarily under the influence of the northern-sourced water, which filled most of the mid-depth to deep Atlantic, while southern-sourced water occasionally occupied the bottom depths (Cronin et al., 1996; Jakob et al., 2021; Lang et al., 2016; Zhang et al., 2013). Although the 41-kyr world Pacific might have seen deep water formation in the subarctic North Pacific (Burls et al., 2017; Ford et al., 2022), this northern-sourced Pacific deep water was limited to depths shallower than 3000 m. Antarctic-sourced bottom water is thought to have covered most of the deep Pacific below 3000 m (Burls et al., 2017; Ford et al., 2022), the depths within which most high-resolution Pacific cores in our compilation belong. The only two high-resolution Pacific cores retrieved from sites shallower than 3000 m in our compilation, ODP 1143 and 1241, display different benthic $\delta^{18}O$ patterns than the deeper cores (Figs. S3-4), possibly because they were under the influence of NPDW instead of southern-sourced PDW. Therefore, the circulation regimes of the two oceans during the 41-kyr world are consistent with sensitivity to antiphase hemispheric insolation forcing during 1.8-1.9 Ma.

Deleted: Perhaps related to the depth of the boundary between NPDW and southern-sourced PDW, the only two high-resolution Pacific cores retrieved from sites shallower than 3000 m, ODP 1143 and 1241, display different benthic $\delta^{18}O$ patterns than the deeper cores (Figs. S3-4).

Our assertion that precession played a role with obliquity in affecting the 41-kyr world glacial cycles joins an array of previous studies reaching similar conclusions. An early study observed a persistent response to precession in 0-5.3 Ma benthic $\delta^{18}O$ after accounting for a long-term trend in $\delta^{18}O$ variance (Lisiecki & Raymo, 2007). Another study detected a nontrivial precession contribution to benthic $\delta^{18}O$ variability from 1-3 Ma using Empirical Nonlinear Orbital Fitting (Liautaud et al., 2020). More recently, precessional influence during the 41-kyr world has been shown in sedimentary elemental records (Sun et al., 2021), sea level (Vaucher et al., 2021), ice-rafted debris (Barker et al., 2022), and ice sheet modeling (Watanabe et al., 2023). Compared to the existing evidence, our finding suggests that benthic $\delta^{18}O$ – the data originally used to demonstrate the "41-kyr problem" (Raymo & Nisancioglu, 2003) – responds to precession forcing differently depending on geographical locations between 1.8-1.9 Ma, possibly due to the different source regions of deep water masses.

Our findings provide potential explanations to previous studies, including Wilkens et al. (2021), that found benthic $\delta^{18}O$ anomalies during 1.8-1.9 Ma. For example, the LR04-aligned benthic $\delta^{18}O$ record and modeled ice volume differed more than normal during 1.8-1.9 Ma (Liautaud et al., 2020 Fig. 4b), probably a result of the LR04 distortion of the glacial cycle features from 1.8-1.9 Ma. Similarly, the difference between the tuned LR04 age model and the untuned, depth-derived age model reaches its maximum just prior to the 1.8-1.9 Ma period (Lisiecki, 2010 Fig. S1).

During the 1.8-1.9 Ma period of strong precession forcing, a Laurentide meltwater event similar to or even larger in magnitude than those in the late Pleistocene has been found in the Gulf of Mexico (Shakun et al., 2016). The alignment of the Gulf of Mexico core in our Atlantic stack (Fig. S7, bottom panel) suggests that this meltwater event occurred during MIS 71 immediately before the very weak glacial maximum in the Atlantic. Terrestrial deposits along the Mississippi River dated to 1.8-2.0 Ma additionally substantiate the size and timing of this Gulf of Mexico meltwater drainage event (Rovey II & Spoering, 2020), indicating the rapid loss of the Laurentide ice similar to meltwater events during the last deglaciation (Barber et al., 1999; Tarasov & Peltier, 2005). As this early Pleistocene meltwater event coincides with one of the weakest obliquity maxima of the 41-kyr world, it suggests sensitivity of the Laurentide ice sheet to precession forcing. Additionally, the meltwater event may have directly or indirectly contributed to the weaker Atlantic benthic $\delta^{18}O$ response during MIS 70.

The modern global ocean oxygen isotope mixing time of about 1500 years (Broecker & Peng, 1983; Rohling, 2013) is too short to explain benthic $\delta^{18}O$ gradients that persist on orbital timescales (Morée et al., 2021). Average deep water mixing times between the Atlantic and Pacific could have been slower during the 41-kyr world and particularly following a large meltwater input to the North Atlantic such as the one discussed above. However, regional variations in benthic $\delta^{18}O$ values do not require slow or uneven mixing of glacial meltwater. For example, regional differences observed in the amplitude of benthic $\delta^{18}O$ change during the last interglacial period (MIS 5) are presumably due to temperature or salinity gradients between water masses (Lisiecki & Stern, 2016). During the 41-kyr world, the amplitude of global ice volume change is smaller in magnitude such that potential regional gradients in deep water temperature or salinity might constitute a larger percentage of the benthic $\delta^{18}O$ signal. The apparently weak benthic $\delta^{18}O$ response during MIS 70 could also be accentuated by dissolution of benthic foraminiferal calcite in the Atlantic if the preceding meltwater event prolonged the residence time of North Atlantic Deep Water, but dissolution is unlikely to fully account for the Atlantic-Pacific discrepancy (Text S3).

Future Directions

Here we attribute the regional benthic $\delta^{18}O$ divergence to the effects of deep water temperature and/or salinity because we are unable to differentiate the impacts of temperature and salinity using only benthic $\delta^{18}O$. However, a bottom water temperature record from the Atlantic shows that deep water temperature and benthic $\delta^{18}O$ co-vary during 1.8-1.9 Ma (Sosdian & Rosenthal, 2009), possibly hinting at the important influence of bottom water temperature on Atlantic benthic $\delta^{18}O$ during this period. As far as we are aware, there is not a commensurate Pacific deep water temperature record that can resolve glacial-interglacial cycles during 1.8-1.9 Ma. Such a

Deleted: 3

Formatted: Font: Bold

Formatted: Font: Bold

record could shed more light on the role deep water temperature played in the Atlantic-Pacific divergence in benthic $\delta^{18}O$ records.

Regardless of the cause of the Atlantic-Pacific divergence, our results demonstrate that regional benthic $\delta^{18}O$ stacks are preferable to global stacks for age model development by stratigraphic alignment. The LR04 stack was created by performing pairwise alignment on all benthic $\delta^{18}O$ records to a target record. The targets were picked because of their relatively high resolution, low noise, and lack of apparent hiatuses. During 1.8-1.9 Ma, LR04 used two sites, ODP 677 and 849, to construct two stacks and observed that the resulting stack was largely independent of the target used. However, both sites 677 and 849 are from the Pacific, which our analysis show are quite dissimilar to Atlantic $\delta^{18}O$ records between 1.8-1.9 Ma. The poor fit between Atlantic records and the Pacific targets likely resulted in localized alignment errors for the Atlantic records.

The delicate task of choosing the right target cores for alignment is alleviated by HMM-stack and BIGMACS (Ahn et al., 2017; Lee and Rand et al., 2023). These software packages align records to a target but iteratively update the alignment target to incorporate information from all other cores, thus reducing the reliance on the user-specified target. Although the iterative approach of BIGMACS was sufficient to identify a difference between the Atlantic and Pacific stacks without tie points (Fig. 1), using the LR04 stack as our initial guess for the regional stacks resulted in ambiguous alignments and distortion of the glacial cycle features from 1.8-1.9 Ma. Ultimately, we resolved this issue by manually creating tie points between glacial maxima and obliquity minima between 1.8-1.9 Ma for the benthic $\delta^{18}O$ records in which the glacial maxima could be confidently identified (Fig. S7).

Deleted: []

Deleted: 3

Conclusion

Benthic $\delta^{18}O$ from five Ceara Rise sites was shown to differ from LR04 global benthic $\delta^{18}O$ stack between 1.8-1.9 Ma (Wilkens et al., 2017). Our investigation reveals that discrepancy with the LR04 stack is widespread over this time interval; most Atlantic $\delta^{18}O$ records show a different pattern of Marine Isotope Stages than Pacific $\delta^{18}O$ records during 1.8-1.9 Ma. The largest difference between the Atlantic and Pacific benthic $\delta^{18}O$ stacks occurs during MIS 70 at ~1.878 Ma, and 1.8-1.9 Ma is the only portion of the Pleistocene for which glacial cycles in the regional stacks differ substantially from LR04 (Fig. 1). The next largest regional difference is an isotopic substage between MIS 77 and 78 at ~2.05 Ma that is warmer in the Atlantic than Pacific. Throughout the rest of the Pleistocene, the Atlantic and Pacific regional stacks agree with LR04 and ProbStack (Fig. 1).

A re-examination of the LR04 construction process shows that the Pacific target cores used as alignment targets from 1.8-1.9 Ma explains why the LR04 stack more closely resembles the Pacific records and produced misalignments of the Atlantic records. This example demonstrates why regional benthic $\delta^{18}O$ stacks are preferable to global stacks for age model development by stratigraphic alignment. The new stacking software BIGMACS facilitates construction of regional stacks by requiring fewer records to generate a stack, but it still has some sensitivity to the choice of initial alignment target. The regional stacks presented here have largely inherited the age model of the LR04 orbital tuning, and updated regional age models, particularly from 1.8-1.9 Ma, should be developed based on these results.

We propose that the cause of the Atlantic-Pacific divergence from 1.8-1.9 Ma is hemispheric sensitivity to antiphased precession forcing, specifically that Atlantic benthic $\delta^{18}O$ at this time was more sensitive to NH summer insolation while deep Pacific benthic $\delta^{18}O$ was more sensitive to SH summer insolation. This benthic $\delta^{18}O$ discrepancy could be caused by variations in the temperature or salinity of northern- versus southern-source deep water rather than requiring uneven mixing of meltwater inputs. The unusually strong precession power and weak obliquity power of orbital cycles from 1.8-1.9 Ma and a contemporaneous meltwater event in the Gulf of Mexico lend support to the Antiphase Hypothesis as a possible mechanism to explain spatial variability in benthic $\delta^{18}O$ during this portion of the 41-kyr world. Our study joins a variety of previous studies (Barker et al., 2022; Liautaud et al., 2020; Lisiecki & Raymo, 2007; Sun et al., 2021; Vaucher et al., 2021; Watanabe et al., 2023) that suggest precession, in addition to obliquity, plays a role in pacing climate signals during the 41-kyr world.

Moved (insertion) [1]

Moved up [1]: (Barker et al., 2022; Liautaud et al., 2020; Lisiecki & Raymo, 2007; Sun et al., 2021; Vaucher et al., 2021; Watanabe et al., 2023)

Acknowledgements

This study benefited from discussions with Devin Rand and Bethany Hobart. This research was funded in part by the Heising-Simons Foundation grant number 2021–2799. Use was made of computational facilities purchased with funds from the National Science Foundation (CNS-1725797) and administered by the Center for Scientific Computing (CSC). The CSC is supported by the California NanoSystems Institute and the Materials Research Science and Engineering Center (MRSEC; NSF DMR 2308708) at UC Santa Barbara. We would like to acknowledge high-performance computing support from Casper (doi:10.5065/D6RX99HX) provided by NCAR's Computational and Information Systems Laboratory, sponsored by the National Science Foundation.

References

Ahn, S., Khider, D., Lisiecki, L. E., & Lawrence, C. E. (2017). A probabilistic Pliocene–Pleistocene stack of benthic $\delta^{18}O$ using a profile hidden Markov model. *Dynamics and Statistics of the Climate System*, *2*(1). https://doi.org/10.1093/climsys/dzx002

Barber, D. C., Dyke, A., Hillaire-Marcel, C., Jennings, A. E., Andrews, J. T., Kerwin, M. W., et al. (1999). Forcing of the cold event of 8,200 years ago by catastrophic drainage of Laurentide lakes. *Nature*, *400*(6742), 344–348. https://doi.org/10.1038/22504

Barker, S., Starr, A., van der Lubbe, J., Doughty, A., Knorr, G., Conn, S., et al. (2022). Persistent influence of precession on northern ice sheet variability since the early Pleistocene. *Science*, *376*(6596), 961–967. https://doi.org/10.1126/science.abm4033

Broecker, W. S., & Peng, T.-H. (1983). *Tracers in the sea*. https://doi.org/10.1016/0016-7037(83)90075-3

Burls, N. J., Fedorov, A. V., Sigman, D. M., Jaccard, S. L., Tiedemann, R., & Haug, G. H. (2017). Active Pacific meridional overturning circulation (PMOC) during the warm Pliocene. *Science Advances*, *3*(9), e1700156. https://doi.org/10.1126/sciadv.1700156

Cronin, T. M., Raymo, M. E., & Kyle, K. P. (1996). Pliocene (3.2–2.4 Ma) ostracode faunal cycles and deep ocean circulation, North Atlantic Ocean. *Geology*, *24*(8), 695–698. https://doi.org/10.1130/0091-7613(1996)024<0695:PMOFCA>2.3.CO;2

Ford, H. L., Burls, N. J., Jacobs, P., Jahn, A., Caballero-Gill, R. P., Hodell, D. A., & Fedorov, A. V. (2022). Sustained mid-Pliocene warmth led to deep water formation in the North Pacific. *Nature Geoscience*, *15*(8), 658–663. https://doi.org/10.1038/s41561-022-00978-3

Hodell, D. A., & Channell, J. E. T. (2016). Mode transitions in Northern Hemisphere glaciation: co-evolution of millennial and orbital variability in Quaternary climate. *Climate of the Past*, *12*(9), 1805–1828. https://doi.org/10.5194/cp-12-1805-2016

Jakob, K. A., Pross, J., Link, J. M., Blaser, P., Hauge Braaten, A., & Friedrich, O. (2021). Deep-ocean circulation in the North Atlantic during the Plio-Pleistocene intensification of Northern Hemisphere Glaciation (~2.65–2.4 Ma). *Marine Micropaleontology*, *165*, 101998. https://doi.org/10.1016/j.marmicro.2021.101998

Khider, D., Emile-Geay, J., Zhu, F., James, A., Landers, J., Ratnakar, V., & Gil, Y. (2022). Pyleoclim: Paleoclimate Timeseries Analysis and Visualization With Python. *Paleoceanography and Paleoclimatology*, *37*(10), e2022PA004509. https://doi.org/10.1029/2022PA004509

Lang, D. C., Bailey, I., Wilson, P. A., Chalk, T. B., Foster, G. L., & Gutjahr, M. (2016). Incursions of southern-sourced water into the deep North Atlantic during late Pliocene glacial intensification. *Nature Geoscience*, *9*(5), 375–379. https://doi.org/10.1038/ngeo2688

Lee, T., Rand, D., Lisiecki, L. E., Gebbie, G., & Lawrence, C. (2023). Bayesian age models and stacks: combining age inferences from radiocarbon and benthic δ^{18}O stratigraphic alignment. *Climate of the Past*, *19*(10), 1993–2012. https://doi.org/10.5194/cp-19-1993-2023

Liautaud, P. R., Hodell, D. A., & Huybers, P. J. (2020). Detection of significant climatic precession variability in early Pleistocene glacial cycles. *Earth and Planetary Science Letters*, *536*, 116137. https://doi.org/10.1016/j.epsl.2020.116137

Lin, L., Khider, D., Lisiecki, L. E., & Lawrence, C. E. (2014). Probabilistic sequence alignment of stratigraphic records. *Paleoceanography*, *29*(10), 976–989. https://doi.org/10.1002/2014PA002713

Lisiecki, L. E. (2010). Links between eccentricity forcing and the 100,000-year glacial cycle. *Nature Geoscience*, *3*(5), 349–352. https://doi.org/10.1038/ngeo828

Lisiecki, L. E., & Raymo, M. E. (2005). A Pliocene-Pleistocene stack of 57 globally distributed benthic $\delta^{18}O$ records. *Paleoceanography*, *20*(1), 1–17. https://doi.org/10.1029/2004PA001071

Lisiecki, L. E., & Raymo, M. E. (2007). Plio–Pleistocene climate evolution: trends and transitions in glacial cycle dynamics. *Quaternary Science Reviews*, *26*(1), 56–69. https://doi.org/10.1016/j.quascirev.2006.09.005

Lisiecki, L. E., & Raymo, M. E. (2009). Diachronous benthic δ18O responses during late Pleistocene terminations. *Paleoceanography*, *24*(3). https://doi.org/10.1029/2009PA001732

Lisiecki, L. E., & Stern, J. V. (2016). Regional and global benthic δ18O stacks for the last glacial cycle. *Paleoceanography*, *31*(10), 1368–1394. https://doi.org/10.1002/2016PA003002

Martinson, D. G., Pisias, N. G., Hays, J. D., Imbrie, J., Moore, T. C., & Shackleton, N. J. (1987). Age Dating and the Orbital Theory of the Ice Ages: Development of a High-Resolution 0 to 300,000-Year Chronostratigraphy. *Quaternary Research*, *27*(1), 1–29. https://doi.org/10.1016/0033-5894(87)90046-9

Morée, A. L., Sun, T., Bretones, A., Straume, E. O., Nisancioglu, K., & Gebbie, G. (2021). Cancellation of the Precessional Cycle in δ18O Records During the Early Pleistocene. *Geophysical Research Letters*, *48*(3), e2020GL090035. https://doi.org/10.1029/2020GL090035

Rasmussen, C. E., & Williams, C. K. I. (2005). *Gaussian Processes for Machine Learning*. Cambridge: MIT Press.

Raymo, M. E., & Nisancioglu, K. H. (2003). The 41 kyr world: Milankovitch's other unsolved mystery. *Paleoceanography*, *18*(1). https://doi.org/10.1029/2002PA000791

Raymo, M. E., Lisiecki, L. E., & Nisancioglu, K. H. (2006). Plio-Pleistocene Ice Volume, Antarctic Climate, and the Global δ18O Record. *Science*, *313*(5786), 492–495. https://doi.org/10.1126/science.1123296

Renaudie, J., Lazarus, D. B., & Diver, P. (2020). NSB (Neptune Sandbox Berlin): An expanded and improved database of marine planktonic microfossil data and deep-sea stratigraphy. *Palaeontologia Electronica*, *23*(1), 1–28. https://doi.org/10.26879/1032

Rohling, E. J. (2013). Oxygen isotope composition of seawater. In *The Encyclopedia of Quaternary Science* (Vol. 2, pp. 915–922). Amsterdam: Elsevier.

Rovey II, C. W., & Spoering, G. (2020). Age and provenance of upland gravels in Missouri, USA, and their relationship to Early Pleistocene glaciation. *Boreas*, *49*(2), 333–349. https://doi.org/10.1111/bor.12429

Shakun, J. D., Raymo, M. E., & Lea, D. W. (2016). An early Pleistocene Mg/Ca-δ18O record from the Gulf of Mexico: Evaluating ice sheet size and pacing in the 41-kyr world. *Paleoceanography*, *31*(7), 1011–1027. https://doi.org/10.1002/2016PA002956

Skinner, L. C., & Shackleton, N. J. (2005). An Atlantic lead over Pacific deep-water change across Termination I: implications for the application of the marine isotope stage stratigraphy. *Quaternary Science Reviews*, *24*(5), 571–580. https://doi.org/10.1016/j.quascirev.2004.11.008

Sosdian, S., & Rosenthal, Y. (2009). Deep-Sea Temperature and Ice Volume Changes Across the Pliocene-Pleistocene Climate Transitions. *Science*, *325*(5938), 306–310. https://doi.org/10.1126/science.1169938

Stern, J. V., & Lisiecki, L. E. (2014). Termination 1 timing in radiocarbon-dated regional benthic δ^{18}O stacks: Regional benthic δ18O stacks. *Paleoceanography*, *29*(12), 1127–1142. https://doi.org/10.1002/2014PA002700

Sun, Y., McManus, J. F., Clemens, S. C., Zhang, X., Vogel, H., Hodell, D. A., et al. (2021). Persistent orbital influence on millennial climate variability through the Pleistocene. *Nature Geoscience*, 1–7. https://doi.org/10.1038/s41561-021-00794-1

Tarasov, L., & Peltier, W. R. (2005). Arctic freshwater forcing of the Younger Dryas cold reversal. *Nature*, *435*(7042), 662–665. https://doi.org/10.1038/nature03617

Torrence, C., & Compo, G. P. (1998). A practical guide to wavelet analysis. *Bull. Am. Meteor. Soc.*, *79*(1), 61–78. https://doi.org/10.1175/1520-0477(1998)079<0061:APGTWA>2.0.CO;2

Vaucher, R., Dashtgard, S. E., Horng, C.-S., Zeeden, C., Dillinger, A., Pan, Y.-Y., et al. (2021). Insolation-paced sea level and sediment flux during the early Pleistocene in Southeast Asia. *Scientific Reports*, *11*(1), 16707. https://doi.org/10.1038/s41598-021-96372-x

Watanabe, Y., Abe-Ouchi, A., Saito, F., Kino, K., O'ishi, R., Ito, T., et al. (2023). Astronomical forcing shaped the timing of early Pleistocene glacial cycles. *Communications Earth & Environment*, *4*(1), 1–11. https://doi.org/10.1038/s43247-023-00765-x

Wilkens, R. H., Westerhold, T., Drury, A. J., Lyle, M., Gorgas, T., & Tian, J. (2017). Revisiting the Ceara Rise, equatorial Atlantic Ocean: isotope stratigraphy of ODP Leg 154 from 0 to 5 Ma. *Climate of the Past*, *13*(7), 779–793. https://doi.org/10.5194/cp-13-779-2017

Zhang, Z.-S., Nisancioglu, K. H., Chandler, M. A., Haywood, A. M., Otto-Bliesner, B. L., Ramstein, G., et al. (2013). Mid-pliocene Atlantic Meridional Overturning Circulation

not unlike modern. *Climate of the Past*, *9*(4), 1495–1504. https://doi.org/10.5194/cp-9-1495-2013